NIH Public Access
Author Manuscript
Circ Res. Author manuscript; available in PMC 2009 July 16.

Published in final edited form as:
Circ Res. 2006 July 21; 99(2): 172–182. doi:10.1161/01.RES.0000232546.92777.05.

Elevated Cytosolic Na^+ Decreases Mitochondrial Ca^{2+} Uptake During Excitation–Contraction Coupling and Impairs Energetic Adaptation in Cardiac Myocytes

Christoph Maack, **Sonia Cortassa**, **Miguel A. Aon**, **Anand N. Ganesan**, **Ting Liu**, and **Brian O'Rourke**
From the Johns Hopkins University, Institute of Molecular Cardiobiology, Division of Cardiology, Baltimore, Md.

Abstract

Mitochondrial Ca^{2+} ($[Ca^{2+}]_m$) regulates oxidative phosphorylation and thus contributes to energy supply and demand matching in cardiac myocytes. Mitochondria take up Ca^{2+} via the Ca^{2+} uniporter (MCU) and extrude it through the mitochondrial Na^+/Ca^{2+} exchanger (mNCE). It is controversial whether mitochondria take up Ca^{2+} rapidly, on a beat-to-beat basis, or slowly, by temporally integrating cytosolic Ca^{2+} ($[Ca^{2+}]_c$) transients. Furthermore, although mitochondrial Ca^{2+} efflux is governed by mNCE, it is unknown whether elevated intracellular Na^+ ($[Na^+]_i$) affects mitochondrial Ca^{2+} uptake and bioenergetics. To monitor $[Ca^{2+}]_m$, mitochondria of guinea pig cardiac myocytes were loaded with rhod-2-acetoxymethyl ester (rhod-2 AM), and $[Ca^{2+}]_c$ was monitored with indo-1 after dialyzing rhod-2 out of the cytoplasm. $[Ca^{2+}]_c$ transients, elicited by voltage-clamp depolarizations, were accompanied by fast $[Ca^{2+}]_m$ transients, whose amplitude (Δ) correlated linearly with $\Delta[Ca^{2+}]_c$. Under β-adrenergic stimulation, $[Ca^{2+}]_m$ decay was ≈2.5-fold slower than that of $[Ca^{2+}]_c$, leading to diastolic accumulation of $[Ca^{2+}]_m$ when amplitude or frequency of $\Delta[Ca^{2+}]_c$ increased. The MCU blocker Ru360 reduced $\Delta[Ca^{2+}]_m$ and increased $\Delta[Ca^{2+}]_c$, whereas the mNCE inhibitor CGP-37157 potentiated diastolic $[Ca^{2+}]_m$ accumulation. Elevating $[Na^+]_i$ from 5 to 15 mmol/L accelerated mitochondrial Ca^{2+} decay, thus decreasing systolic and diastolic $[Ca^{2+}]_m$. In response to gradual or abrupt changes of workload, reduced nicotinamide-adenine dinucleotide (NADH) levels were maintained at 5 mmol/L $[Na^+]_i$, but at 15 mmol/L, the NADH pool was partially oxidized. The results indicate that (1) mitochondria take up Ca^{2+} rapidly and contribute to fast buffering during a $[Ca^{2+}]_c$ transient; and (2) elevated $[Na^+]_i$ impairs mitochondrial Ca^{2+} uptake, with consequent effects on energy supply and demand matching. The latter effect may have implications for cardiac diseases with elevated $[Na^+]_i$.

Keywords

calcium uniporter; Na^+/Ca^{2+} exchange; calcium buffer; energy metabolism; oxidative phosphorylation; Krebs cycle

Copyright © 2006 American Heart Association. All rights reserved.

Correspondence to Brian O'Rourke, PhD, Institute of Molecular Cardiobiology, Division of Cardiology, 720 Rutland Ave, 1059 Ross Bldg, Baltimore, MD 21205-2195. E-mail E-mail: bor@jhmi.edu.
Current address for C.M.: Universität des Saarlandes, Klinik für Innere Medizin III, Homburg/Saar, Germany.

This manuscript was sent to Harry Fozzard, Consulting Editor, for review by expert referees, editorial decision, and final disposition.

Disclosures
None.

NIH-PA Author Manuscript
NIH-PA Author Manuscript
NIH-PA Author Manuscript

NIH-PA Author Manuscript

NIH-PA Author Manuscript

NIH-PA Author Manuscript

Cardiac excitation–contraction (EC) coupling requires enormous amounts of ATP.[1] Mitochondria, which are spatially interleaved with myofibrils and the sarcoplasmic reticulum (SR),[2] are the primary site of ATP production. Two main regulatory factors match mitochondrial ATP production to the constantly varying energy demand of the cell, ADP and Ca^{2+}.[1–6] With increasing workload, ADP and Pi stimulate the F_1F_0-ATPase to produce ATP and consume the proton motive force ($\Delta\mu_H$), leading to stimulation of the electron transport chain and oxidation of reduced nicotinamide-adenine dinucleotide (NADH)[5] (Figure 1). On the other hand, an increase of workload is associated with an increase of time-averaged cytosolic $[Ca^{2+}]$ ($[Ca^{2+}]_c$). Facilitated by the strong electrochemical driving force for Ca^{2+} influx, Ca^{2+} enters mitochondria via the Ca^{2+} uniporter (MCU) and activates 3 key dehydrogenases of the tricarboxylic acid (TCA) cycle.[1,5,7,8] This accelerates the production of NADH, providing a driving force for electrons in the respiratory chain to increase $\Delta\mu_H$ and maintain ATP production.[5] Thus, in response to changes of workload, the complementary regulation of oxidative phosphorylation by ADP and Ca^{2+} maintains cellular ATP and the NADH redox potential.[3–5]

The kinetics of mitochondrial Ca^{2+} uptake in intact cardiac myocytes, however, are not fully resolved.[9] Experiments on isolated mitochondria revealed a relatively low affinity of the MCU for Ca^{2+} ($K_m \approx 10$ to 20 μmol/L).[8,10] Because, in cardiac myocytes, bulk $[Ca^{2+}]_c$ peaks between 0.5 and ≈3 μmol/L, it was proposed that mitochondria do not take up Ca^{2+} rapidly [8,10–12] This view is supported by experimental data from isolated cardiac myocytes[13–16] and ventricular trabeculae,[4,17] where no beat-to-beat changes, but rather a slow increase of mitochondrial $[Ca^{2+}]$ ($[Ca^{2+}]_m$) in response to an increase of the frequency and/or amplitude of $[Ca^{2+}]_c$ transients, was observed. In contrast, other studies[18–22] reported rapid $[Ca^{2+}]_m$ transients that closely followed $[Ca^{2+}]_c$ with similar kinetics.

In this context, the spatiotemporal organization of Ca^{2+}-handling proteins in "microdomains" may be of relevance for mitochondrial Ca^{2+} uptake. In the junctional cleft between L-type Ca^{2+} channels and ryanodine receptors (RyRs) of the SR, $[Ca^{2+}]$ peaks 10 to 20 ms after the onset of the action potential at concentrations of ≈50 to 100 μmol/L.[12,23] This brief "junctional Ca^{2+}" pulse is shaped by the diffusion of Ca^{2+} to the cytosolic bulk space.[23] Experiments on permeabilized myocytes[24] and H9c2 myotubes[25–27] suggested that mitochondria are located ≈40 to 300 nm from the dyadic junction[24] and exposed to $[Ca^{2+}]$ of ≈30 to 50 μmol/L, clearly exceeding bulk $[Ca^{2+}]_c$.[25,27] This concept of a "mitochondrial microdomain" with high $[Ca^{2+}]$ is already well established in various noncardiac cell types, where the close vicinity of mitochondria to inositol 1,4,5-triphosphate (IP_3) receptors of the endoplasmic reticulum allows spatially and temporally organized Ca^{2+} signal transmission and enables mitochondria to shape $[Ca^{2+}]_c$.[28] Conversely, in cardiac myocytes, it is still widely believed that the flux of Ca^{2+} leaving the cytosol by entering mitochondria is inconsequential with respect to EC coupling.[12,14,23] However, the quantitative impact of $[Ca^{2+}]_c$ buffering by mitochondria has neither been fully resolved[14,27] nor has it been assessed in concert with its effects on bioenergetics. Thus, in the present study, we use a novel technique to monitor both $[Ca^{2+}]_c$ and $[Ca^{2+}]_m$ within the same cell to elucidate the kinetics of mitochondrial Ca^{2+} uptake and its consequences for EC coupling.

Furthermore, because mitochondrial Ca^{2+} efflux is governed by the mitochondrial Na^+/Ca^{2+} exchanger (mNCE), we hypothesized that elevated $[Na^+]_i$ may reduce steady-state $[Ca^{2+}]_m$ and consequently affect the regulation of oxidative phosphorylation. Hence, we tested whether elevated $[Na^+]_i$ adversely affects energy supply and demand matching in cardiac cells, with potential implications for cardiac diseases such as hypertrophy and failure,[29–31] in which intracellular $[Na^+]$ ($[Na^+]_i$) is elevated.

NIH-PA Author Manuscript

NIH-PA Author Manuscript

NIH-PA Author Manuscript

Materials and Methods

An expanded Materials and Methods section is in the online data supplement, available at http://circres.ahajournals.org.

Briefly, isolated guinea pig cardiomyocytes were incubated with rhod-2-acetoxymethyl ester (rhod-2 AM) (3 μmol/L) to monitor $[Ca^{2+}]_m$. Using the patch-clamp technique, cytosolic traces of rhod-2 were eliminated by whole-cell dialysis with a pipette solution containing indo-1 (75 μmol/L) to monitor $[Ca^{2+}]_c$. To measure NADH autofluorescence together with $[Ca^{2+}]_m$, myocytes were dialyzed with dye-free pipette solution. To determine $\Delta\Psi_m$, cells were incubated with tetramethyl rhodamine methyl ester (TMRM) (50 nmol/L). $[Ca^{2+}]_c$ transients were elicited by voltage steps from −80 mV to +10 mV at 1 to 4 Hz, in the absence and presence of isoproterenol (1 to 100 nmol/L).

Results

Rapid Kinetics of Mitochondrial Ca^{2+} Uptake

$[Ca^{2+}]_c$ and $[Ca^{2+}]_m$ were recorded in the same cell using the dual dye loading of rhod-2 and indo-1. After pulsing at 1 Hz for 1 minute under control conditions, isoproterenol increased $[Ca^{2+}]_c$ transients (Figure 2A). Notably, even before isoproterenol application, a rapid $[Ca^{2+}]_m$ transient was observed during the $[Ca^{2+}]_c$ transient (Figure 2A through 2D), with an amplitude (Δ) that correlated linearly with $\Delta[Ca^{2+}]_c$ (Figure 3C). Similarly, raising extracellular $[Ca^{2+}]$ from 2 to 8 mmol/L also increased $\Delta[Ca^{2+}]_c$ and $\Delta[Ca^{2+}]_m$ (supplemental Figure VIII). When comparing the kinetics of $[Ca^{2+}]_c$ and $[Ca^{2+}]_m$ transients in the presence of isoproterenol (100 nmol/L; Figure 2E through 2I), the upstroke of the $[Ca^{2+}]_m$ transient preceded that of $[Ca^{2+}]_c$, resulting in a shorter time-to-peak (TTP) of $[Ca^{2+}]_m$ than of $[Ca^{2+}]_c$ (Figure 2F and 2H). In contrast, the decay of $[Ca^{2+}]_m$ was ≈2.5-fold slower than the $[Ca^{2+}]_c$ decay (Figure 2G and 2I). This slower decay of $[Ca^{2+}]_m$ resulted in a stepwise accumulation of diastolic $[Ca^{2+}]_m$ in response to increasing $\Delta[Ca^{2+}]_c$ (Figure 2C), even though diastolic $[Ca^{2+}]_c$ remained constant over the course of the experiment (Figures 2A and 3A).

Inhibiting Mitochondrial Ca^{2+} Uptake

When Ru360, a specific inhibitor of the MCU,[32,33] was added to the pipette solution (10 or 100 nmol/L), $\Delta[Ca^{2+}]_m$ was concentration-dependently decreased (Figure 3B, 3F and 3H), and diastolic accumulation of $[Ca^{2+}]_m$ was blunted (Figure 3B). This was associated with a prolonged TTP, but unchanged rate of decay of $[Ca^{2+}]_m$ (Figure 3G, 3I and 3J). Conversely, the amplitude of $[Ca^{2+}]_c$ transients was enhanced at 10 nmol/L but reduced at 100 nmol/L of Ru360 (Figure 3A, 3E and 3H). The TTP of $[Ca^{2+}]_c$ slightly shortened (Figure 3I), whereas the decay of $[Ca^{2+}]_c$ was prolonged at 100 nmol/L Ru360 (Figure 3E and 3J). At 10 nmol/L Ru360, diastolic $[Ca^{2+}]_c$ was increased by ≈50 nmol/L throughout the experiment (inset in Figure 3A). When $\Delta[Ca^{2+}]_c$ increased in response to isoproterenol, a transient occurrence of extrasystoles induced a reversible increase of diastolic $[Ca^{2+}]_c$ (between 240 and 360 seconds). At 100 nmol/L Ru360, however, these extrasystoles persisted throughout the rest of the experiment in 3 of 7 cells (not shown), resulting in an increase of diastolic $[Ca^{2+}]_c$ by up to ≈200 nmol/L ($P<0.05$; inset in Figure 3A).

In the presence of Ru360, the slope of the linear relationship between $\Delta[Ca^{2+}]_m$ and $\Delta[Ca^{2+}]_c$ was reduced by 64% and 77% for 10 and 100 nmol/L, respectively (Figure 3C). As an estimate of the effects of Ru360 on the steady-state $[Ca^{2+}]_c$ transient amplitude, the Ru360-sensitive component of $\Delta[Ca^{2+}]_c$ was calculated as the difference between $\Delta[Ca^{2+}]_c$ measured in the presence and absence of 10 nmol/L Ru360 ($=\Delta[Ca^{2+}]_{c/Ru360(10\ nmol/L)}-\Delta[Ca^{2+}]_{c/Control}$) and plotted as a function of $\Delta[Ca^{2+}]_{c/Control}$ (Figure 3D). Above a threshold of

NIH-PA Author Manuscript

NIH-PA Author Manuscript

NIH-PA Author Manuscript

$\Delta[Ca^{2+}]_c$=519 nmol/L, the Ru360-sensitive component of $\Delta[Ca^{2+}]_c$ was well fit by the linear function y=0.8×–417 nmol/L.

Inhibiting Mitochondrial Ca^{2+} Efflux

$[Ca^{2+}]_m$ efflux in cardiac cells is governed by the mNCE.[8,10] Intracellular application of CGP-37157 (1 μmol/L), an inhibitor of the mNCE,[34] enhanced $[Ca^{2+}]_m$ accumulation at 3-Hz stimulation frequency (Figure 4B). It is of note that already before initiation of the pulse protocol (after equilibrating the cytosol with CGP-37157 for ≈10 minutes), resting $[Ca^{2+}]_m$ was elevated by 24% compared with control conditions (at time=0, Figure 4B; signals normalized to fluorescence before cell dialysis). Consistent with enhanced buffering of Ca^{2+} in the mitochondrial compartment, $\Delta[Ca^{2+}]_c$ transients were reduced in the presence of CGP-37157 (Figure 4A and 4C). Whereas $[Ca^{2+}]_c$ decay was unaffected by CGP-37157, the $[Ca^{2+}]_m$ decay was prolonged (Figure 4E and 4F).

Increasing Stimulation Frequency

Because $[Ca^{2+}]_m$ decay was ≈2.5-fold slower than $[Ca^{2+}]_c$ decay during β-adrenergic stimulation (Figure 2G and 2I), the stimulation frequency would be expected to have an important impact on diastolic accumulation of $[Ca^{2+}]_m$. In fact, at 3 Hz, diastolic accumulation of $[Ca^{2+}]_m$ was substantially more pronounced than at 1 Hz (at comparable $[Ca^{2+}]_c$; supplemental Figure IX).

Elevating $[Na^+]_i$

Because the mNCE governs mitochondrial Ca^{2+} efflux[8,10] (Figure 4), and $[Na^+]_i$ is increased in various cardiac disease states,[29–31] we tested whether elevating $[Na^+]_i$ would affect $[Ca^{2+}]_c$ and $[Ca^{2+}]_m$. Increasing $[Na^+]_i$ from 5 to 15 mmol/L in the pipette solution increased $\Delta[Ca^{2+}]_c$ ≈1.4- to 1.5-fold in control conditions or in the presence of low concentrations of isoproterenol. At 100 nmol/L isoproterenol, the enhancement of $\Delta[Ca^{2+}]_c$ by $[Na^+]_i$ was less evident, as expected because the SR Ca^{2+} load would be high with maximal β-adrenergic stimulation (supplemental Figure X; Figure 5A, 5E and 5H). In contrast to the effect on $\Delta[Ca^{2+}]_c$, elevated $[Na^+]_i$ decreased the amplitude of the $[Ca^{2+}]_m$ transients (Figure 5B, 5F and 5H). This was associated with a longer TTP but a faster decay of $[Ca^{2+}]_m$ at higher $[Na^+]_i$ (Figure 5G, 5I and 5J). Consequently, diastolic accumulation of $[Ca^{2+}]_m$ was blunted (Figure 5B). Both the slope of the correlation between $\Delta[Ca^{2+}]_m$ and $\Delta[Ca^{2+}]_c$ (Figure 5C) and the Ru360-sensitive component of $\Delta[Ca^{2+}]_c$ and $[Ca^{2+}]_c$ were reduced (Figure 5D), indicating that for any given $[Ca^{2+}]_c$ transient, less Ca^{2+} entered the mitochondria at higher $[Na^+]_i$.

Similar results were obtained when 5 and 15 mmol/L $[Na^+]_i$ were compared at a higher stimulation frequency (3 Hz; Figure 6A and 6B; supplemental Figure XI). The relative decrease in $\Delta[Ca^{2+}]_m$ by higher $[Na^+]_i$ was less pronounced at 3 Hz (−35%; supplemental Figure XIE and XIG) compared with 1-Hz stimulation (−66%; Figure 5F and 5H). Again, inhibiting the mNCE with CGP-37157 (1 μmol/L) increased resting $[Ca^{2+}]_m$ and potentiated accumulation of diastolic $[Ca^{2+}]_m$ (supplemental Figure XII).

Implications for Mitochondrial Energetics

To estimate the consequences of reduced $[Ca^{2+}]_m$ for mitochondrial energetics, we determined the redox state of NADH/NAD^+ (Figure 6C) and $\Delta\Psi_m$ (Figure 6D) using the same protocol as used for $[Ca^{2+}]_c$ and $[Ca^{2+}]_m$ (3 Hz; Figure 6A and 6B). At 5 mmol/L $[Na^+]_i$, NADH was well maintained during the protocol (Figure 6C). In contrast, at 15 mmol/L $[Na^+]_i$, net oxidation of NADH occurred when workload increased in response to isoproterenol. NADH remained partially oxidized throughout the rest of the experiment at 15 mmol/L $[Na^+]_i$. In contrast, $\Delta\Psi_m$ was unaffected by β-adrenergic stimulation at either 5 or 15 mmol/L $[Na^+]_i$ (Figure 6D).

NIH-PA Author Manuscript

NIH-PA Author Manuscript

NIH-PA Author Manuscript

To induce a more abrupt change in workload, we superfused resting myocytes with isoproterenol (100 nmol/L) and then paced cells at 4 Hz for 100 seconds (Figure 7A) or 200 seconds (Figure 7B and 7C). At 5 mmol/L $[Na^+]_i$, pacing increased both systolic and diastolic $[Ca^{2+}]_m$ (Figure 7A, top). At the onset of stimulation, rapid oxidation of NADH occurred ("undershoot"), followed by recovery of NADH in parallel with increasing $[Ca^{2+}]_m$ (Figure 7A). After cessation of stimulation, an "overshoot" of NADH was observed, followed by a gradual recovery toward the initial resting level. The recovery was preceded by a decline of $[Ca^{2+}]_m$.

The stimulation protocol was extended to 200 seconds to allow more time for NADH recovery. At 15 mmol/L $[Na^+]_i$, mitochondrial Ca^{2+} uptake was blunted (Figure 7B and 7C, upper panels). The initial oxidation of NADH was potentiated, and the recovery of NADH was blunted or absent at higher $[Na^+]_i$ (Figure 7B and 7C, lower panels). In contrast, at 5 mmol/L $[Na^+]_i$, NADH was maintained, which was related to a less pronounced undershoot and a more prominent recovery of NADH after the onset of work.

Discussion

The key findings of the present study are that (1) mitochondria take up Ca^{2+} rapidly and buffer $[Ca^{2+}]_c$ during EC coupling; (2) the kinetics of mitochondrial Ca^{2+} uptake are compatible with the concept of a "mitochondrial microdomain"[24–28]; and (3) elevating $[Na^+]_i$ reduces mitochondrial Ca^{2+} uptake, which impairs the matching process of energy supply and demand by oxidizing the NADH/NAD^+ redox potential.

Rapid Mitochondrial Ca^{2+} Transients

During each $[Ca^{2+}]_c$ transient, a rapid $[Ca^{2+}]_m$ transient occurred. Contamination of the mitochondrial signal by cytosolic traces of rhod-2 was eliminated by equilibrating the cytoplasm with rhod-2–free pipette solution (see the online data supplement). The amplitude of the $[Ca^{2+}]_m$ transient was linearly correlated with $\Delta[Ca^{2+}]_c$, indicating a close association between mitochondrial Ca^{2+} uptake and SR Ca^{2+} release. The MCU inhibitor Ru360 (10 nmol/L) reduced $\Delta[Ca^{2+}]_m$ and prolonged its TTP, whereas it increased $\Delta[Ca^{2+}]_c$ (Figure 3). Conversely, the mNCE inhibitor CGP-37157 prolonged the decay of $[Ca^{2+}]_m$, but not of $[Ca^{2+}]_c$, and elevated diastolic $[Ca^{2+}]_m$ (Figure 4). These findings strongly support the contention that rhod-2 selectively reported changes in mitochondrial matrix Ca^{2+}, the net effect of Ca^{2+} uptake via the MCU and Ca^{2+} efflux through the mNCE. Concerning the rapid beat-to-beat changes of $[Ca^{2+}]_m$ during EC coupling, the results differ from some previous studies[13–17] but are in general agreement with others.[18–22]

Mitochondrial Ca^{2+}-Uptake Kinetics

In the present study, the peak of $[Ca^{2+}]_m$ preceded the peak of $[Ca^{2+}]_c$ by ≈20 ms during β-adrenergic stimulation. It is rather unlikely that this observation is related to differential dye kinetics or buffering capacities of the mitochondrial matrix compared with the cytosol (as discussed in the online data supplement). Although previous studies reported rapid $[Ca^{2+}]_m$ transients during EC coupling,[18–22] none of them observed $[Ca^{2+}]_m$ transients preceding $[Ca^{2+}]_c$ transients. In contrast, $[Ca^{2+}]_m$ transients typically followed the $[Ca^{2+}]_c$ transients with a lag of ≈20 to 50 ms. The reasons for this discrepancy are unclear, but in all but one[22] of these studies, $[Ca^{2+}]_c$ and $[Ca^{2+}]_m$ were not collected at the same time or in the same cell, and the temporal resolution of the signals was low, making it difficult to compare kinetics directly.

Other studies did not observe beat-to-beat changes of $[Ca^{2+}]_m$ during $[Ca^{2+}]_c$ transients at all.[13–17] In most of those studies,[13–16] $[Ca^{2+}]_m$ was reported by indo-1 AM, and cytosolic indo-1 was quenched with $MnCl_2$. However, Mn^{2+} competes with Ca^{2+} for the MCU and may be

NIH-PA Author Manuscript

NIH-PA Author Manuscript

NIH-PA Author Manuscript

taken up into mitochondria as well.[4,10] This could quench mitochondrial indo-1 and possibly inhibit the MCU. Because the mNCE is also inhibited by Mn^{2+},[10] mitochondrial Ca^{2+}-transport kinetics may have been perturbed under these conditions. Moreover, in 1 study[16] using the Mn^{2+}-quench method, $[Ca^{2+}]_c$ was raised by reverse-mode Na^+/Ca^{2+} exchange, which is unlikely to increase Ca^{2+} in the vicinity of the mitochondria as much, or as quickly, as SR Ca^{2+} release.[12,16,23]

Mitochondrial Ca^{2+}-Decay Kinetics

The decay of $[Ca^{2+}]_m$ was ≈2.5-fold slower than the decay of $[Ca^{2+}]_c$ (in the presence of isoproterenol). An increase of amplitude (Figures 2 through 6) or frequency (supplemental Figure IX) of $[Ca^{2+}]_c$ transients led to a stepwise accumulation of diastolic $[Ca^{2+}]_m$. In response to β-adrenergic stimulation, SR Ca^{2+}-ATPase velocity is substantially accelerated by protein kinase A (PKA)-mediated phosphorylation of phospholamban,[12] whereas acceleration of mNCE activity has not been reported.[8,10] Accordingly, in our experiments, decay of $[Ca^{2+}]_c$, but not $[Ca^{2+}]_m$, was accelerated by isoproterenol (supplemental Figure VII). This differential regulation of SR Ca^{2+}-ATPase and mNCE may be of physiological importance, because in vivo, β-adrenergic stimulation increases both the amplitude and frequency of $[Ca^{2+}]_c$ transients. Under these conditions, shortening of the $[Ca^{2+}]_c$ transient, but not the $[Ca^{2+}]_m$ transient, facilitates a stepwise increase of diastolic $[Ca^{2+}]_m$ with important bioenergetic consequences (see below), whereas diastolic $[Ca^{2+}]_c$, and thus diastolic (and systolic) function of the heart, is maintained.

Differences in the decay kinetics for $[Ca^{2+}]_c$ and $[Ca^{2+}]_m$ transients have not been reported in previous studies.[18–22] Only 1 study observed a short-term increase of diastolic $[Ca^{2+}]_m$, with no change in diastolic $[Ca^{2+}]_c$ after the application of isoproterenol. In most other reports, an increase in diastolic $[Ca^{2+}]_m$ was associated with a concordant increase in diastolic $[Ca^{2+}]_c$.[13,15,21] In contrast, in studies reporting slow mitochondrial Ca^{2+}-uptake kinetics, accumulation of $[Ca^{2+}]_m$ during changes in $\Delta[Ca^{2+}]_c$ amplitude or frequency[4,13,15] resembled the diastolic increase of $[Ca^{2+}]_m$ in the present study.

Evidence for a Mitochondrial Ca^{2+} Microdomain

In cardiac myocytes, different subcellular microdomains display substantially different Ca^{2+} concentrations and kinetics.[12,23] Ca^{2+} enters the cell through L-type Ca^{2+} channels ($I_{Ca,L}$), triggering SR Ca^{2+} release into the junctional cleft (Ca^{2+}-induced Ca^{2+} release [CICR]) via the ryanodine receptor (RyR2 subtype).[12] This induces a brief junctional Ca^{2+} transient that reaches ≈50 to 100 μmol/L.[12,23] Junctional Ca^{2+} decays rapidly by diffusing into the bulk cytosol ($[Ca^{2+}]_c$), where it peaks later and at much lower concentrations than in the cleft.[23] Because indo-1 reports $[Ca^{2+}]_c$ primarily from the bulk phase, the earlier peak of $[Ca^{2+}]_m$ compared with $[Ca^{2+}]_c$ in our study indicates that mitochondria may sense an early increase of $[Ca^{2+}]$ in a microdomain that is closer to the SR Ca^{2+}-release sites than the bulk cytosol. In fact, electron micrographs show that most mitochondria are located within 40 to 300 nm from the dyad and may be exposed to $[Ca^{2+}]$ in the range of 30 to 50 μmol/L,[24,25,27] which would be sufficient to activate the MCU (K_m for Ca^{2+}≈10 to 20 μmol/L).[8,10]

Although the molecular identity of the MCU is still unresolved, and other Ca^{2+}-transporting systems in the inner mitochondrial membrane have been proposed (see the online data supplement for detailed discussion), we investigated whether our experimental results could be reproduced in a computer model of mitochondrial bioenergetics and Ca^{2+} handling[5] without modifying the basic formulations of the MCU and mNCE. Pulses of Ca^{2+} resembling those expected to be encountered in a mitochondrial Ca^{2+} microdomain[23–25] ($[Ca^{2+}]_{MD}$) were simulated with an exogenous Ca^{2+} spike function with peak $[Ca^{2+}]$ of either 10 or 20 μmol/L for a duration of 50 ms (Figure 8D). These pulses of $[Ca^{2+}]_{MD}$ elicited rapid $[Ca^{2+}]_m$ transients.

NIH-PA Author Manuscript

NIH-PA Author Manuscript

NIH-PA Author Manuscript

An increase of either $[Ca^{2+}]_{MD}$ amplitude (Figure 8A) or frequency (Figure 8B) independently increased diastolic $[Ca^{2+}]_m$. An increase in both amplitude and frequency of the pulses potentiated diastolic $[Ca^{2+}]_m$ accumulation (Figure 8C). These simulations are in qualitative agreement with our experimental results and lend support to the hypothesis that mitochondria sense $[Ca^{2+}]$ in a microdomain, rather than the bulk $[Ca^{2+}]_c$. This interpretation is consistent with reports that caffeineinduced $[Ca^{2+}]_m$ transients[24,25] or mitochondrial Ca^{2+} sparks ("Ca^{2+} marks")[26] can be observed even when the diffusion of Ca^{2+} released from the SR is restricted by the presence of exogenous Ca^{2+} buffers.

Influence of Mitochondrial Ca^{2+} Uptake on EC Coupling

In the present study, partial inhibition of mitochondrial Ca^{2+} uptake by Ru360 increased the amplitude of $[Ca^{2+}]_c$ transients and slightly elevated diastolic $[Ca^{2+}]_c$. Similar effects were observed in mouse myocytes treated with Ru360[35] or shortly after dissipation of $\Delta\Psi_m$ with mitochondrial uncouplers.[18] In our experiments, above a threshold of $\Delta[Ca^{2+}]_c$=519 nmol/L, the Ru360-sensitive component of $\Delta[Ca^{2+}]_c$ followed the equation y=0.8×–417 nmol/L (Figure 3D). If we consider that 10 nmol/L Ru360 inhibits $\Delta[Ca^{2+}]_m$ by 66% at a $\Delta[Ca^{2+}]_c$ of 1 μmol/L, we estimate that the beat-dependent rapid buffering effect of mitochondria decreases the steady-state $[Ca^{2+}]_c$ transients by ≈36%. A previous report determined that mitochondria buffer ≈26% of the Ca^{2+} released from the SR in H9c2 myotubes.[27] However, other studies,[12,14,36] including our own,[37] suggested that mitochondria contribute only ≈1% to the removal of $[Ca^{2+}]_c$. The latter studies focused on the removal of $[Ca^{2+}]_c$ well after Ca^{2+} was released from the SR, perhaps not taking into account that mitochondria might already take up Ca^{2+} during the early phase of SR Ca^{2+} release.[24–26]

As a technical limitation, it should be noted that the indirect assessment of Ca^{2+} taken up by mitochondria (Figure 3D) based on the Ru360 effects relies on comparisons of $[Ca^{2+}]_c$ in unpaired cells and under steady-state conditions. Furthermore, because rhod-2 as an indicator for $[Ca^{2+}]_m$ was not calibrated, the current results do not allow a precise quantification of the magnitude of the fluxes across the inner mitochondrial membrane on each beat. Further studies will have to clarify these quantitative aspects in more detail.

Nevertheless, rapid buffering of $[Ca^{2+}]_c$ by mitochondria is likely to play an important physiological role, because in a recent study, mitochondrial Ca^{2+} uptake preserved "local control" by preventing the propagation of SR Ca^{2+} release after caffeine application in mouse myocytes.[35] In this context, our observation that the frequency of extrasystoles increased in the presence of isoproterenol and Ru360 (Figure 3A) warrants further investigation as to whether impaired mitochondrial Ca^{2+} uptake could contribute to arrhythmias.

Bioenergetic Consequences of Mitochondrial Ca^{2+} Uptake

To elucidate the bioenergetic consequences of mitochondrial Ca^{2+} uptake during EC coupling, we measured NADH together with $[Ca^{2+}]_m$. When $[Ca^{2+}]_c$ transients were gradually increased by cumulatively increasing isoproterenol, the redox state of NADH was maintained at 5 mmol/L $[Na^+]_i$ (Figure 6C). However, when an abrupt change of workload was simulated by pacing myocytes at 4 Hz in the presence of isoproterenol, NADH was initially oxidized, followed by a recovery phase that paralleled mitochondrial Ca^{2+} uptake (Figure 7). In previous studies, Brandes and Bers[3,4] observed a similar phenomenon in rat cardiac trabeculae, which could be reproduced by computational modeling.[5] These findings can be explained by the abrupt increase of work initiating ATP hydrolysis, which increases the availability of ADP and P_i to stimulate ATP production by the F_1F_0-ATPase at the expense of $\Delta\mu_H$ (see also Figure 1). Consumption of $\Delta\mu_H$ (rather than an increase of $[Ca^{2+}]_m$; see also the online data supplement) immediately stimulates electron transport, proton pumping, and the rate of NADH oxidation at the onset of work (Figure 7A, bottom). At the same time, the increase of amplitude and

NIH-PA Author Manuscript

NIH-PA Author Manuscript

NIH-PA Author Manuscript

frequency of $[Ca^{2+}]_c$ transients promotes mitochondrial Ca^{2+} uptake (Figure 7A, top), activating key dehydrogenases of the TCA cycle to facilitate (re-)reduction of oxidized NAD^+.[1,5,7,8] This explains the recovery of NADH in parallel with the $[Ca^{2+}]_m$ increase[3–5] (Figure 7A, bottom). When workload is withdrawn, the availability of ADP to the F_1F_0-ATPase abruptly decreases, and the rate of NADH oxidation decreases. Because $[Ca^{2+}]_m$ is still elevated, the turnover of the TCA cycle remains increased, producing the typical overshoot of NADH (Figure 7A, bottom). NADH normalizes when $[Ca^{2+}]_m$ decreases back to baseline.

Effect of Elevated $[Na^+]_i$ on Cytosolic and Mitochondrial $[Ca^{2+}]$

The physiological range of $[Na^+]_i$ in resting cardiac myocytes is ≈5 to 15 mmol/L and is species dependent.[31] Whereas in small animals with high heart rates (ie, mice and rats), $[Na^+]_i$ is 10 to 15 mmol/L, larger animals (including guinea pigs) have $[Na^+]_i$ between 5 and 10 mmol/L.[31] Under physiological conditions, $[Na^+]_i$ rises by several millimoles per liter in response to an increase of heart rate.[30,38] Under pathological conditions, $[Na^+]_i$ is elevated at all stimulation frequencies in cardiac hypertrophy and failure.[29–31]

An increase of $[Na^+]_i$ increases SR Ca^{2+} load (and thus $\Delta[Ca^{2+}]_c$) by decreasing forward-mode Ca^{2+} extrusion and enhancing reverse-mode Na^+/Ca^{2+}-exchange activity during the action potential.[29,39,40] In our experiments, elevation of $[Na^+]_i$ from 5 to 15 mmol/L increased $\Delta[Ca^{2+}]_c$≈1.5-fold under basal conditions, or at low concentrations of isoproterenol (supplemental Figure X). This increase was similar to previous studies showing an approximate doubling of $\Delta[Ca^{2+}]_c$ in $[Na^+]_i$-loaded cells at 1 Hz.[39,41] The effect of high $[Na^+]_i$ on $\Delta[Ca^{2+}]_c$ was less pronounced during maximal β-adrenergic stimulation, because SR Ca^{2+} load is expected to be already near-maximally elevated (supplemental Figure X).

Increasing $[Na^+]_i$ from 5 to 15 mmol/L accelerated the decay of $[Ca^{2+}]_m$, which is presumably related to an increased electrochemical gradient driving the exchange of cytosolic Na^+ for intramitochondrial Ca^{2+} via the mNCE (K_d for $[Na^+]_i$≈5 to 12 mmol/L[5,42,43]) and is consistent with experiments on isolated mitochondria.[43,44] Unexpectedly, the upstroke velocity and amplitude of $[Ca^{2+}]_m$ transients were substantially decreased. In simulations of $[Ca^{2+}]_m$ dynamics defined by fast uptake through the MCU and slower efflux through the mNCE (Figure 8), the effect of high $[Na^+]_i$ on the rising phase of the $[Ca^{2+}]_m$ transient could not be reproduced by acceleration of mNCE alone. Understanding this finding will require further investigation (several possibilities are discussed in the online data supplement).

The effects of elevated $[Na^+]_i$ on the amplitude and decay velocity of $[Ca^{2+}]_m$ transients resulted in decreased diastolic accumulation of $[Ca^{2+}]_m$ (Figure 5B). Keeping in mind the frequency dependence of $[Na^+]_i$,[30,38] a physiological implication of this observation in vivo may be that increased $[Na^+]_i$ at higher heart rates prevents mitochondrial Ca^{2+} overload, potentially protecting mitochondria from a permeability transition and cell death.[45] In this context, the higher resting $[Na^+]_i$ in species with higher heart rates may play a similar role. For example, rapid $[Ca^{2+}]_m$ transients have been observed in intact guinea pig, but not rat cardiac myocytes.[46]

Effect of Elevated $[Na^+]_i$ on Mitochondrial Energetics

The basal redox state of mitochondrial NADH was not different at 5 versus 15 mmol/L $[Na^+]_i$. However, when workload was increased either continuously (Figure 6) or abruptly (Figure 7), NADH was partially oxidized at 15 mmol/L $[Na^+]_i$, whereas it was maintained at 5 mmol/L $[Na^+]_i$. The underlying mechanism is presumably a lack of Ca^{2+}-induced stimulation of TCA cycle dehydrogenases attributable to less mitochondrial Ca^{2+} uptake at higher $[Na^+]_i$.

NIH-PA Author Manuscript

NIH-PA Author Manuscript

NIH-PA Author Manuscript

Conclusions

The results of our study suggest that during EC coupling, elevated $[Na^+]_i$ reduces rapid mitochondrial Ca^{2+} uptake and oxidizes the NADH/NAD^+ redox potential. In the failing heart, $[Na^+]_i$ is elevated,[29–31] and SR Ca^{2+} release is decreased. According to our results, both processes would diminish mitochondrial Ca^{2+} uptake and NADH production. On the other hand, elevated heart rate and increased preload may increase the energy demand of the failing heart. We propose that this energetic mismatch may contribute to energy starvation of the failing heart,[47] which eventually leads to progressive myocardial injury and decompensation of cardiac function.

Supplementary Material

Refer to Web version on PubMed Central for supplementary material.

Acknowledgments

Sources of Funding

This work was supported by NIH grants R01 HL61711 and P50 HL-52307 (to B.O'R.). C.M. is supported by the Deutsche Forschungsgemeinschaft (Emmy Noether-Programm).

References

1. Balaban RS. Cardiac energy metabolism homeostasis: role of cytosolic calcium. J Mol Cell Cardiol 2002;34:1259–1271. [PubMed: 12392982]
2. Territo PR, French SA, Dunleavy MC, Evans FJ, Balaban RS. Calcium activation of heart mitochondrial oxidative phosphorylation: rapid kinetics of mVO2, NADH, AND light scattering. J Biol Chem 2001;276:2586–2599. [PubMed: 11029457]
3. Brandes R, Bers DM. Intracellular Ca2+ increases the mitochondrial NADH concentration during elevated work in intact cardiac muscle. Circ Res 1997;80:82–87. [PubMed: 8978326]
4. Brandes R, Bers DM. Simultaneous measurements of mitochondrial NADH and Ca(2 +) during increased work in intact rat heart trabeculae. Biophys J 2002;83:587–604. [PubMed: 12124250]
5. Cortassa S, Aon MA, Marban E, Winslow RL, O'Rourke B. An integrated model of cardiac mitochondrial energy metabolism and calcium dynamics. Biophys J 2003;84:2734–2755. [PubMed: 12668482]
6. Saks VA, Kuznetsov AV, Vendelin M, Guerrero K, Kay L, Seppet EK. Functional coupling as a basic mechanism of feedback regulation of cardiac energy metabolism. Mol Cell Biochem 2004;256–257:185–199.
7. Gunter TE, Gunter KK, Sheu SS, Gavin CE. Mitochondrial calcium transport: physiological and pathological relevance. Am J Physiol 1994;267:C313–C339. [PubMed: 8074170]
8. Denton RM, McCormack JG. Ca2+ transport by mammalian mitochondria and its role in hormone action. Am J Physiol 1985;249:E543–E554. [PubMed: 2417490]
9. Huser J, Blatter LA, Sheu SS. Mitochondrial calcium in heart cells: beat-to-beat oscillations or slow integration of cytosolic transients? J Bioenerg Biomembr 2000;32:27–33. [PubMed: 11768759]
10. Gunter TE, Pfeiffer DR. Mechanisms by which mitochondria transport calcium. Am J Physiol 1990;258:C755–C786. [PubMed: 2185657]
11. Hansford RG. Relation between mitochondrial calcium transport and control of energy metabolism. Rev Physiol Biochem Pharmacol 1985;102:1–72. [PubMed: 2863864]
12. Bers DM. Cardiac excitation-contraction coupling. Nature 2002;415:198–205. [PubMed: 11805843]
13. Miyata H, Silverman HS, Sollott SJ, Lakatta EG, Stern MD, Hansford RG. Measurement of mitochondrial free Ca2+ concentration in living single rat cardiac myocytes. Am J Physiol 1991;261:H1123–H1134. [PubMed: 1928394]

NIH-PA Author Manuscript

NIH-PA Author Manuscript

NIH-PA Author Manuscript

14. Bassani RA, Bassani JW, Bers DM. Mitochondrial and sarcolemmal Ca2+ transport reduce [Ca2+]i during caffeine contractures in rabbit cardiac myocytes. J Physiol 1992;453:591–608. [PubMed: 1464847]
15. Di Lisa F, Gambassi G, Spurgeon H, Hansford RG. Intramitochondrial free calcium in cardiac myocytes in relation to dehydrogenase activation. Cardiovasc Res 1993;27:1840–1844. [PubMed: 8275533]
16. Zhou Z, Matlib MA, Bers DM. Cytosolic and mitochondrial Ca2+ signals in patch clamped mammalian ventricular myocytes. J Physiol 1998;507(pt 2):379–403. [PubMed: 9518700]
17. Moravec CS, Bond M. Effect of inotropic stimulation on mitochondrial calcium in cardiac muscle. J Biol Chem 1992;267:5310–5316. [PubMed: 1544913]
18. Isenberg G, Han S, Schiefer A, Wendt-Gallitelli MF. Changes in mitochondrial calcium concentration during the cardiac contraction cycle. Cardiovasc Res 1993;27:1800–1809. [PubMed: 8275527]
19. Chacon E, Ohata H, Harper IS, Trollinger DR, Herman B, Lemasters JJ. Mitochondrial free calcium transients during excitation-contraction coupling in rabbit cardiac myocytes. FEBS Lett 1996;382:31–36. [PubMed: 8612759]
20. Trollinger DR, Cascio WE, Lemasters JJ. Selective loading of Rhod 2 into mitochondria shows mitochondrial Ca2+ transients during the contractile cycle in adult rabbit cardiac myocytes. Biochem Biophys Res Commun 1997;236:738–742. [PubMed: 9245725]
21. Ohata H, Chacon E, Tesfai SA, Harper IS, Herman B, Lemasters JJ. Mitochondrial Ca2+ transients in cardiac myocytes during the excitationcontraction cycle: effects of pacing and hormonal stimulation. J Bioenerg Biomembr 1998;30:207–222. [PubMed: 9733088]
22. Robert V, Gurlini P, Tosello V, Nagai T, Miyawaki A, Di Lisa F, Pozzan T. Beat-to-beat oscillations of mitochondrial [Ca2+] in cardiac cells. EMBO J 2001;20:4998–5007. [PubMed: 11532963]
23. Shannon TR, Wang F, Puglisi J, Weber C, Bers DM. A mathematical treatment of integrated Ca dynamics within the ventricular myocyte. Biophys J 2004;87:3351–3371. [PubMed: 15347581]
24. Sharma VK, Ramesh V, Franzini-Armstrong C, Sheu SS. Transport of Ca2+ from sarcoplasmic reticulum to mitochondria in rat ventricular myocytes. J Bioenerg Biomembr 2000;32:97–104. [PubMed: 11768767]
25. Szalai G, Csordas G, Hantash BM, Thomas AP, Hajnoczky G. Calcium signal transmission between ryanodine receptors and mitochondria. J Biol Chem 2000;275:15305–15313. [PubMed: 10809765]
26. Pacher P, Thomas AP, Hajnoczky G. Ca2+ marks: miniature calcium signals in single mitochondria driven by ryanodine receptors. Proc Natl Acad Sci USA 2002;99:2380–2385. [PubMed: 11854531]
27. Pacher P, Csordas P, Schneider T, Hajnoczky G. Quantification of calcium signal transmission from sarco-endoplasmic reticulum to the mitochondria. J Physiol 2000;529(pt 3):553–564. [PubMed: 11118489]
28. Rizzuto R, Duchen MR, Pozzan T. Flirting in little space: the ER/mitochondria Ca2+ liaison. Sci STKE 2004;2004re1
29. Despa S, Islam MA, Weber CR, Pogwizd SM, Bers DM. Intracellular Na(+) concentration is elevated in heart failure but Na/K pump function is unchanged. Circulation 2002;105:2543–2548. [PubMed: 12034663]
30. Pieske B, Maier LS, Piacentino V 3rd, Weisser J, Hasenfuss G, Houser S. Rate dependence of [Na+] i and contractility in nonfailing and failing human myocardium. Circulation 2002;106:447–453. [PubMed: 12135944]
31. Pieske B, Houser SR. [Na+]i handling in the failing human heart. Cardiovasc Res 2003;57:874–886. [PubMed: 12650866]
32. Matlib MA, Zhou Z, Knight S, Ahmed S, Choi KM, Krause-Bauer J, Phillips R, Altschuld R, Katsube Y, Sperelakis N, Bers DM. Oxygen-bridged dinuclear ruthenium amine complex specifically inhibits Ca2+ uptake into mitochondria in vitro and in situ in single cardiac myocytes. J Biol Chem 1998;273:10223–10231. [PubMed: 9553073]
33. Kirichok Y, Krapivinsky G, Clapham DE. The mitochondrial calcium uniporter is a highly selective ion channel. Nature 2004;427:360–364. [PubMed: 14737170]
34. Cox DA, Conforti L, Sperelakis N, Matlib MA. Selectivity of inhibition of Na(+)-Ca2+ exchange of heart mitochondria by benzothiazepine CGP-37157. J Cardiovasc Pharmacol 1993;21:595–599. [PubMed: 7681905]

NIH-PA Author Manuscript

NIH-PA Author Manuscript

NIH-PA Author Manuscript

35. Seguchi H, Ritter M, Shizukuishi M, Ishida H, Chokoh G, Nakazawa H, Spitzer KW, Barry WH. Propagation of Ca2+ release in cardiac myocytes: role of mitochondria. Cell Calcium 2005;38:1–9. [PubMed: 15993240]
36. Bassani JW, Bassani RA, Bers DM. Ca2+ cycling between sarcoplasmic reticulum and mitochondria in rabbit cardiac myocytes. J Physiol 1993;460:603–621. [PubMed: 8387590]
37. Hobai IA, O'Rourke B. Enhanced Ca(2+)-activated Na(+)-Ca(2+) exchange activity in canine pacing-induced heart failure. Circ Res 2000;87:690–698. [PubMed: 11029405]
38. Cohen CJ, Fozzard HA, Sheu SS. Increase in intracellular sodium ion activity during stimulation in mammalian cardiac muscle. Circ Res 1982;50:651–662. [PubMed: 7074728]
39. Armoundas AA, Hobai IA, Tomaselli GF, Winslow RL, O'Rourke B. Role of sodium-calcium exchanger in modulating the action potential of ventricular myocytes from normal and failing hearts. Circ Res 2003;93:46–53. [PubMed: 12805237]
40. Weber CR, Piacentino V 3rd, Houser SR, Bers DM. Dynamic regulation of sodium/calcium exchange function in human heart failure. Circulation 2003;108:2224–2229. [PubMed: 14557358]
41. Mubagwa K, Lin W, Sipido K, Bosteels S, Flameng W. Monensin-induced reversal of positive force-frequency relationship in cardiac muscle: role of intracellular sodium in rest-dependent potentiation of contraction. J Mol Cell Cardiol 1997;29:977–989. [PubMed: 9152859]
42. Bers DM, Barry WH, Despa S. Intracellular Na+ regulation in cardiac myocytes. Cardiovasc Res 2003;57:897–912. [PubMed: 12650868]
43. Paucek P, Jaburek M. Kinetics and ion specificity of Na(+)/Ca(2+) exchange mediated by the reconstituted beef heart mitochondrial Na(+)/Ca(2+) antiporter. Biochim Biophys Acta 2004;1659:83–91. [PubMed: 15511530]
44. Cox DA, Matlib MA. A role for the mitochondrial Na(+)-Ca2+ exchanger in the regulation of oxidative phosphorylation in isolated heart mitochondria. J Biol Chem 1993;268:938–947. [PubMed: 8419373]
45. Brookes PS, Yoon Y, Robotham JL, Anders MW, Sheu SS. Calcium, ATP, and ROS: a mitochondrial love-hate triangle. Am J Physiol Cell Physiol 2004;287:C817–C833. [PubMed: 15355853]
46. Griffiths EJ. Species dependence of mitochondrial calcium transients during excitation-contraction coupling in isolated cardiomyocytes. Biochem Biophys Res Commun 1999;263:554–559. [PubMed: 10491330]
47. Ingwall JS, Weiss RG. Is the failing heart energy starved? On using chemical energy to support cardiac function. Circ Res 2004;95:135–145. [PubMed: 15271865]

NIH-PA Author Manuscript

NIH-PA Author Manuscript

NIH-PA Author Manuscript

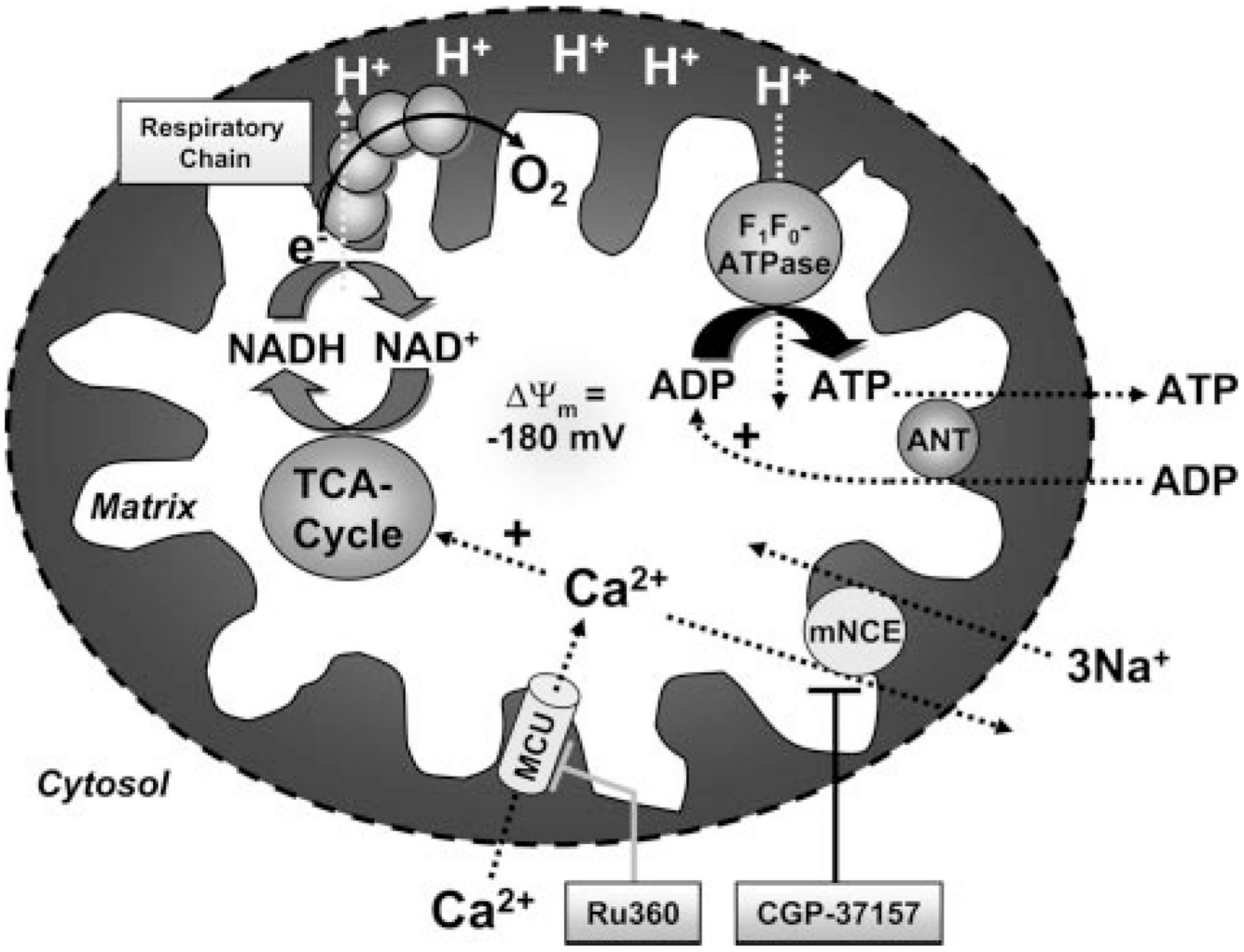

Figure 1.

Key processes of mitochondrial energetics including NADH production by the TCA cycle, oxidative phosphorylation, and their regulation by Ca^{2+} and ADP. ANT indicates adeninenucleotide translocator.

NIH-PA Author Manuscript
NIH-PA Author Manuscript
NIH-PA Author Manuscript

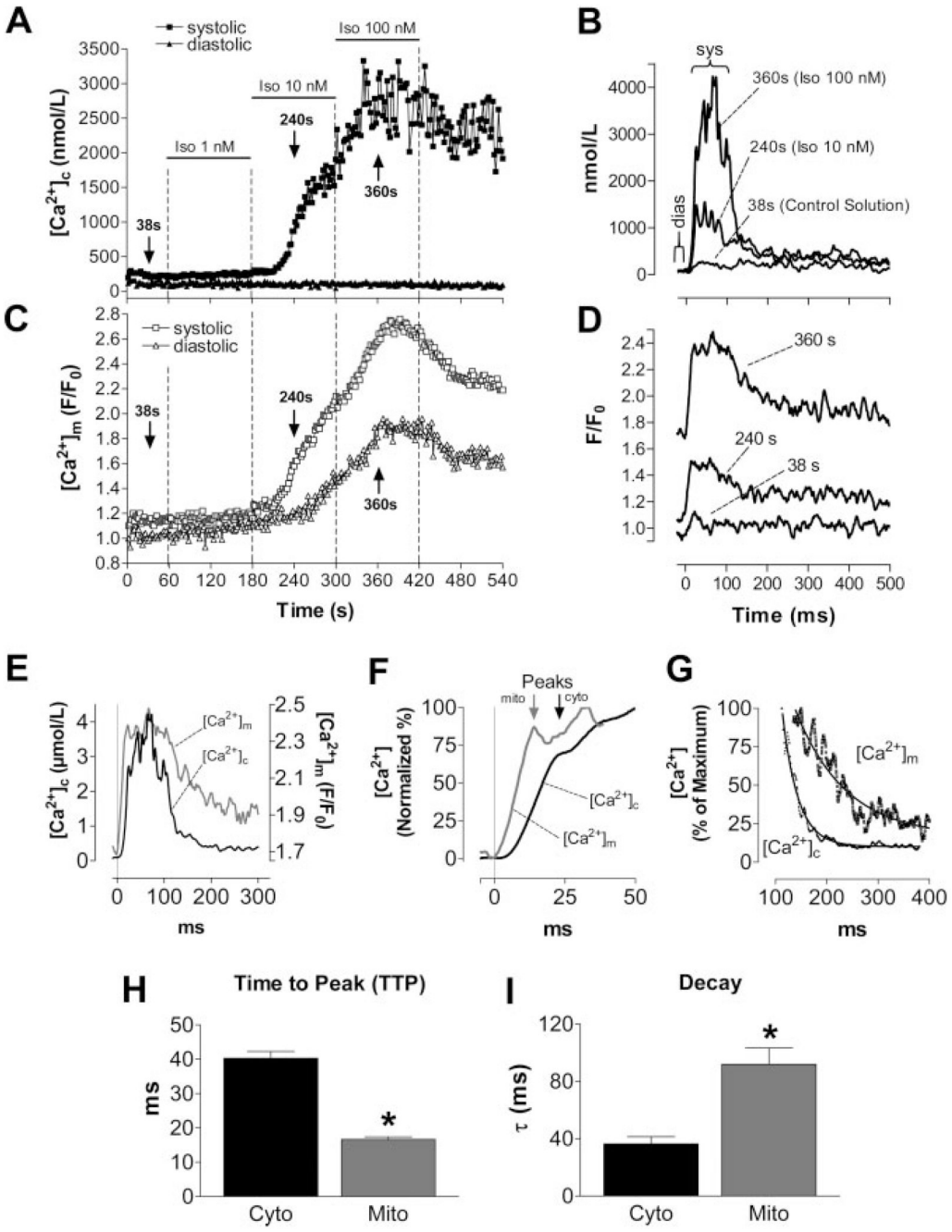

Figure 2.

Representative experiment determining $[Ca^{2+}]_c$ and $[Ca^{2+}]_m$ in the same cell. $[Ca^{2+}]_c$ transients were elicited at 1 Hz in the absence and presence of isoproterenol (Iso; 1 to 100 nmol/L) (A and C). The $[Ca^{2+}]$ transients in B and D were recorded at the indicated time points of the protocol (arrows in A and C). E through G, $[Ca^{2+}]_c$ and $[Ca^{2+}]_m$ transients at 100 nmol/L isoproterenol. H and I, Aggregate data for TTP and the exponential time constant, τ, for the decay of $[Ca^{2+}]_c$ and $[Ca^{2+}]_m$, respectively. *P<0.0001 vs $[Ca^{2+}]_c$ (n=10).

NIH-PA Author Manuscript
NIH-PA Author Manuscript
NIH-PA Author Manuscript

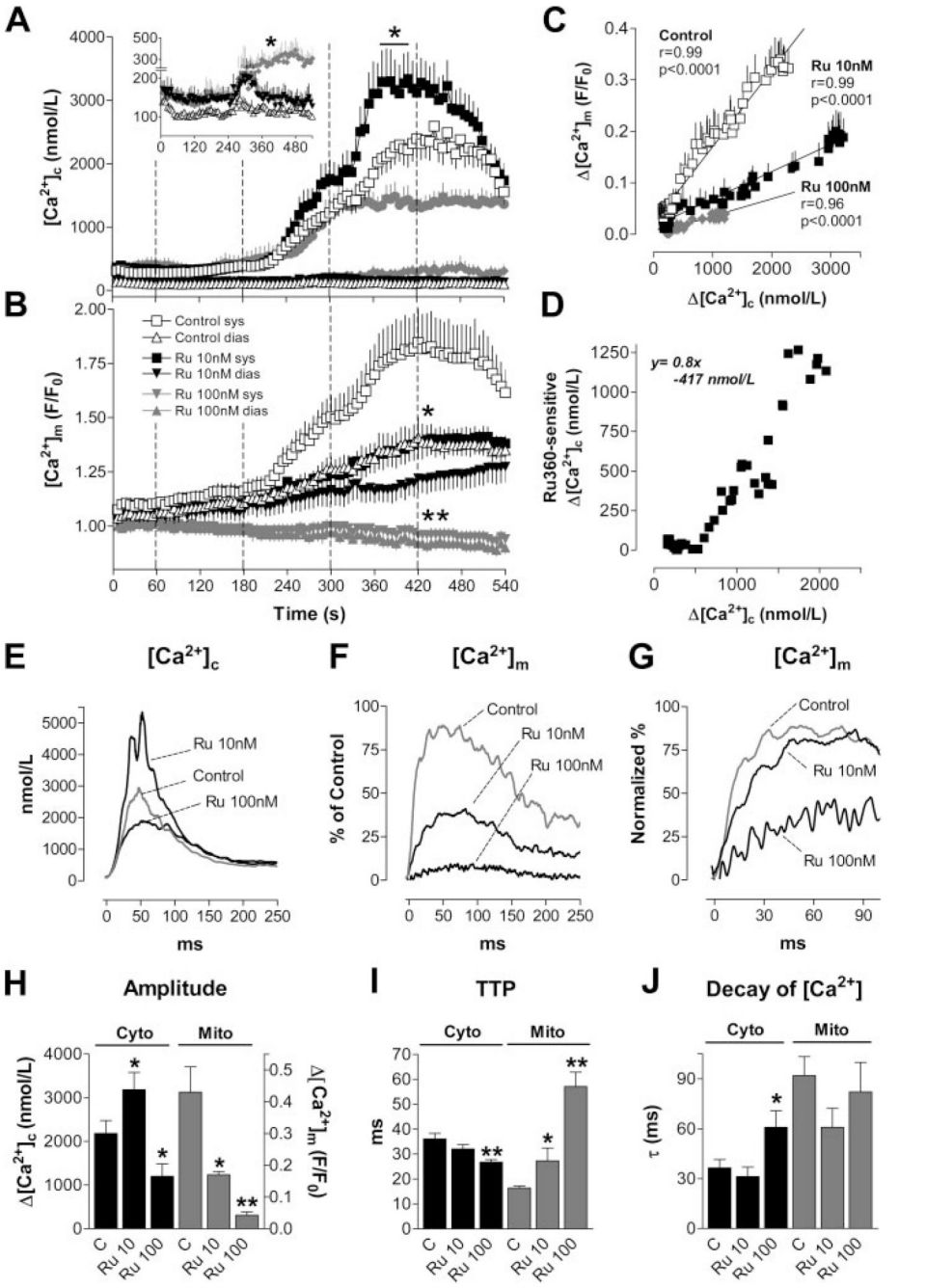

Figure 3.

A and B, $[Ca^{2+}]_c$ and $[Ca^{2+}]_m$ in the absence (Control; A, cytosolic, n=20; B, mitochondrial, n=10) or presence of Ru360 (10 nmol/L, n=15/8; 100 nmol/L, n=7/7). Dotted lines indicate the switch of superfusing solutions (isoproterenol, 1 to 100 nmol/L) as indicated in Figure 2A. Inset in A, Diastolic $[Ca^{2+}]_c$ at higher resolution. C and D, $\Delta[Ca^{2+}]_m$ (C) or Ru360-sensitive $\Delta[Ca^{2+}]_c$ (D; $=\Delta[Ca2+]_{c/Ru360(10\ nmol/L)}-\Delta[Ca^{2+}]_{c/Control}$), plotted against $\Delta[Ca^{2+}]_c$, respectively. E through J, Aggregate results for $[Ca^{2+}]$ transient kinetics in the absence (Control, n=10) or presence of Ru360 (10 nmol/L, n=8; 100 nmol/L, n=7). E and F, Amplitudes of $[Ca^{2+}]_c$ and $[Ca^{2+}]_m$ transients. G, Normalized values for $[Ca^{2+}]_m$ transients. SEM omitted

NIH-PA Author Manuscript

NIH-PA Author Manuscript

NIH-PA Author Manuscript

for clarity. H through J, Amplitude, TTP, and τ for decay of $[Ca^{2+}]_c$ and $[Ca^{2+}]_m$ transients, respectively. **P*<0.05, ***P*<0.01 vs control.

NIH-PA Author Manuscript
NIH-PA Author Manuscript
NIH-PA Author Manuscript

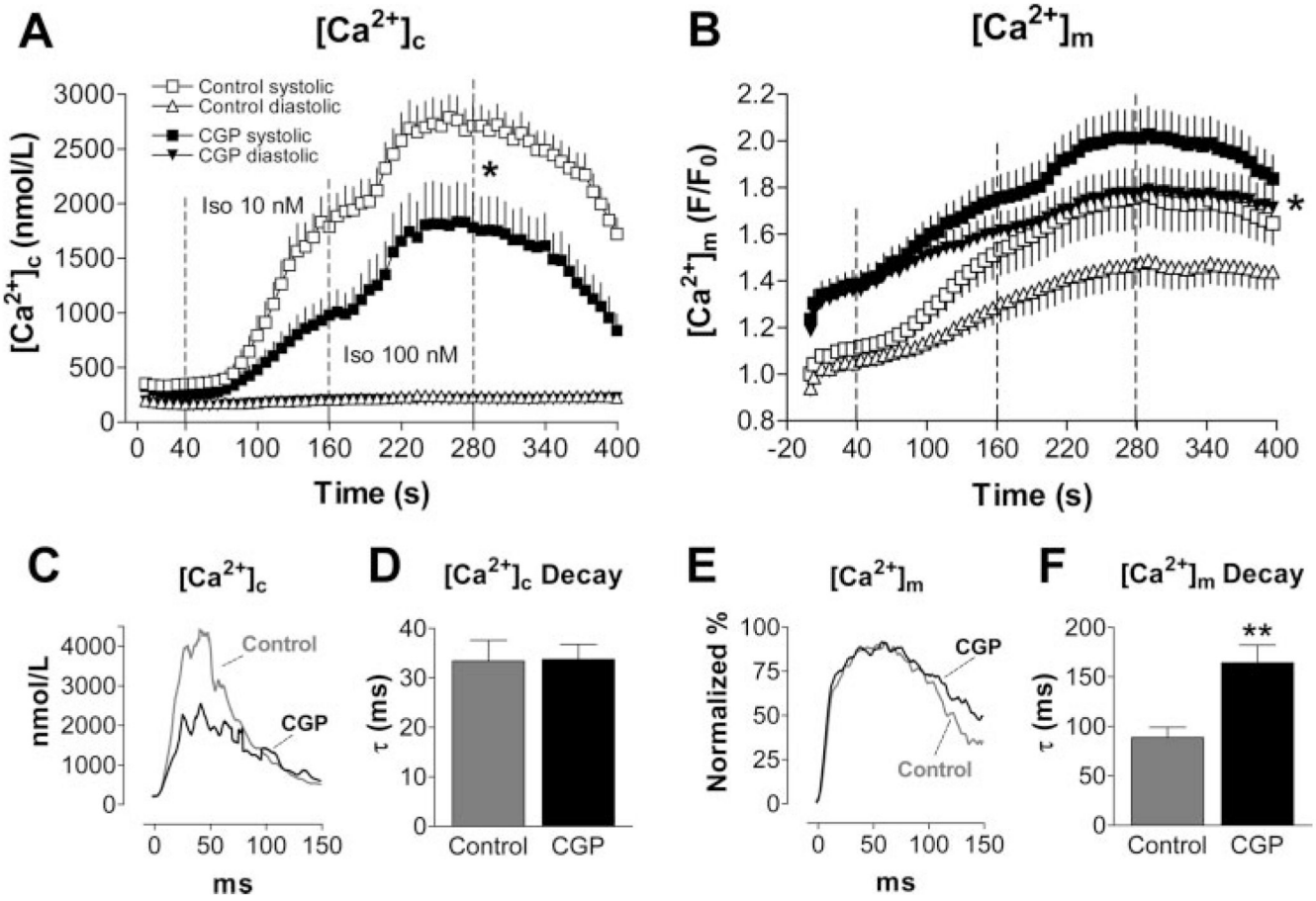

Figure 4.

$[Ca^{2+}]_c$ and $[Ca^{2+}]_m$ at 3-Hz stimulation frequency in the absence (Control; n = 16) or presence of CGP-37157 (intracellular application, 1 μmol/L; n = 15), respectively. Average $[Ca^{2+}]_c$ or $[Ca^{2+}]_m$ plotted against the time of the whole experiment (A and B) or the time of a single transient at 100 nmol/L isoproterenol (C and E; SEM omitted for clarity). Average time constant (τ) of the rate of decay of $[Ca^{2+}]_c$ (D) or $[Ca^{2+}]_m$ (F), respectively. **P*<0.05, ***P*<0.0001 vs control.

NIH-PA Author Manuscript
NIH-PA Author Manuscript
NIH-PA Author Manuscript

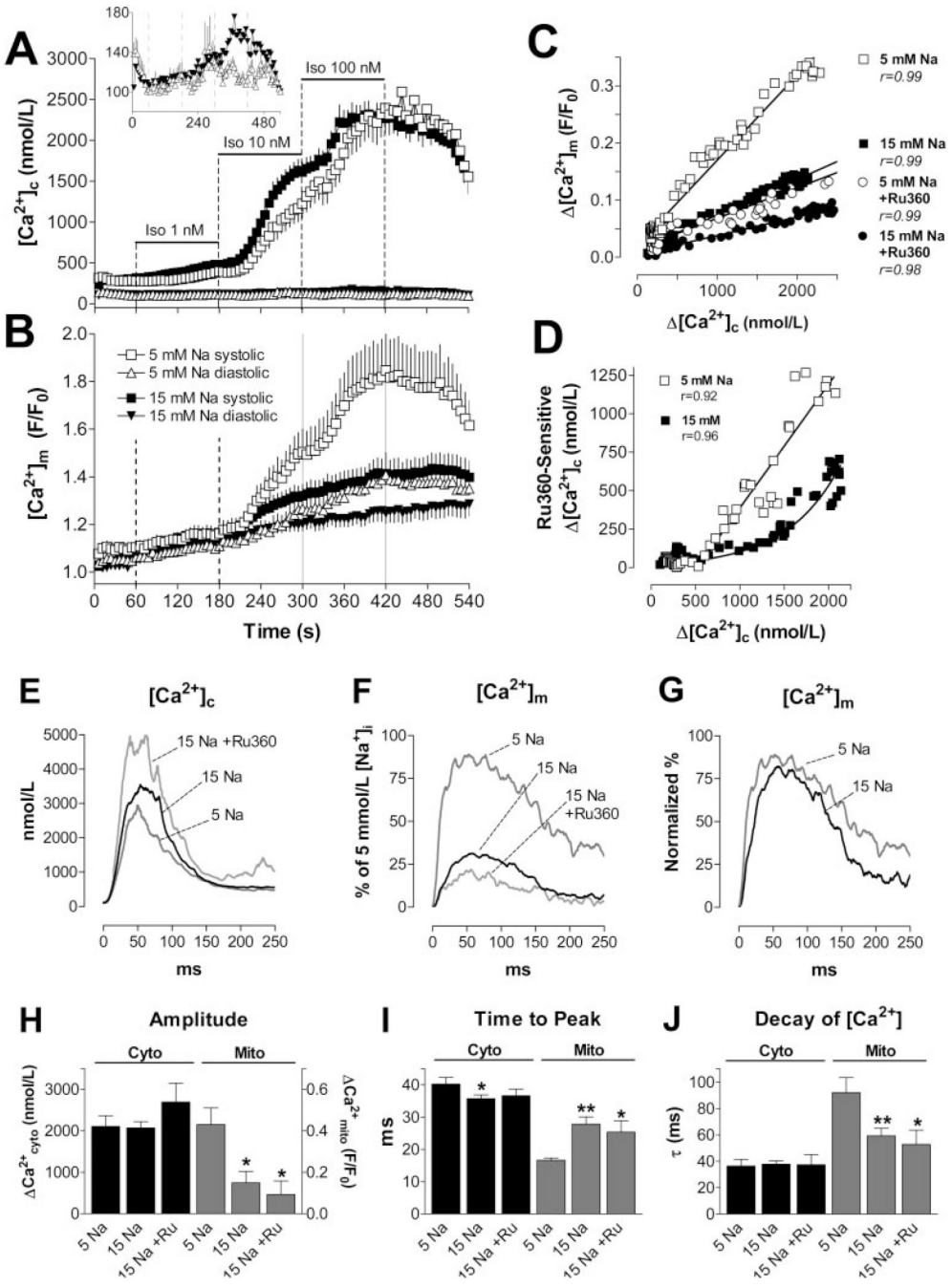

Figure 5.

A and B, $[Ca^{2+}]_c$ (A: 5 mmol/L $[Na^+]_i$, n=20; 15 mmol/L $[Na^+]_i$, n=46) and $[Ca^{2+}]_m$ transients (B: n = 10/24) at 1 Hz. Inset in A, Diastolic $[Ca^{2+}]_c$ at higher resolution. C, $\Delta[Ca^{2+}]_m$ plotted against $\Delta[Ca^{2+}]_c$ at 5 and 15 mmol/L $[Na^+]_i$ in the absence and presence of Ru360 (10 nmol/L), respectively. D, Ru360-sensitive $\Delta[Ca^{2+}]_c$ (as in Figure 3D) plotted against $\Delta[Ca^{2+}]_c$ at 5 and 15 mmol/L $[Na^+]_i$. E through J, Kinetics of $[Ca^{2+}]_c$ and $[Ca^{2+}]_m$ transients at 5 mmol/L $[Na^+]_i$ (n=10) and 15 mmol/L $[Na^+]_i$ in the absence (n=21) or presence of Ru360 (10 nmol/L; n=9). H through J, Amplitude, TTP, and τ for decay of $[Ca^{2+}]_c$ and $[Ca^{2+}]_m$, respectively. **P*<0.05; ***P*<0.01 vs 5 mmol/L $[Na^+]_i$.

NIH-PA Author Manuscript
NIH-PA Author Manuscript
NIH-PA Author Manuscript

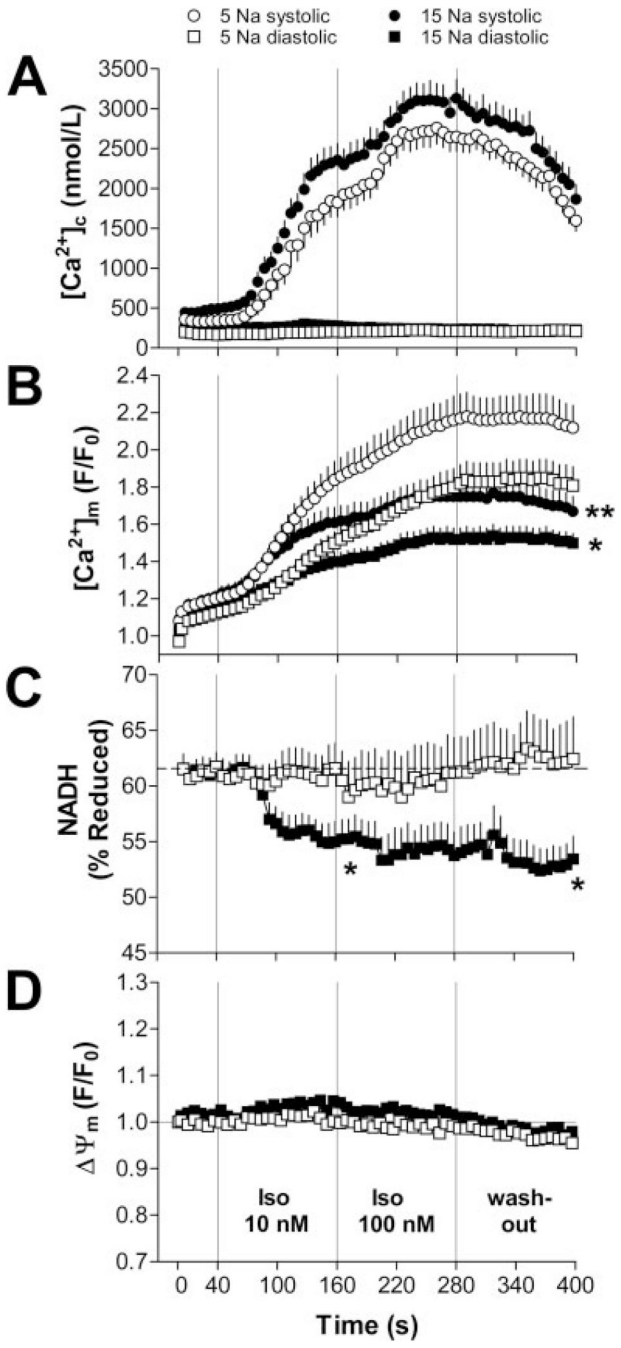

Figure 6.

$[Ca^{2+}]_c$ (A: 5 mmol/L $[Na^+]_i$, n=29; 15 mmol/L $[Na^+]_i$, n=38), $[Ca^{2+}]_m$ (B: n=32/45), NADH (C: n=13/14), and $\Delta\psi_m$ (D: n=8/7) in myocytes paced at 3 Hz. Note that data were not collected in the same cells, but as combinations of either $[Ca^{2+}]_c$/ $[Ca^{2+}]_m$, $[Ca^{2+}]_m$/NADH, or $\Delta\psi_m$/ $[Ca^{2+}]_c$ (see Materials and Methods). *P<0.05, **P<0.01 vs 5 mmol/L $[Na^+]_i$.

NIH-PA Author Manuscript
NIH-PA Author Manuscript
NIH-PA Author Manuscript

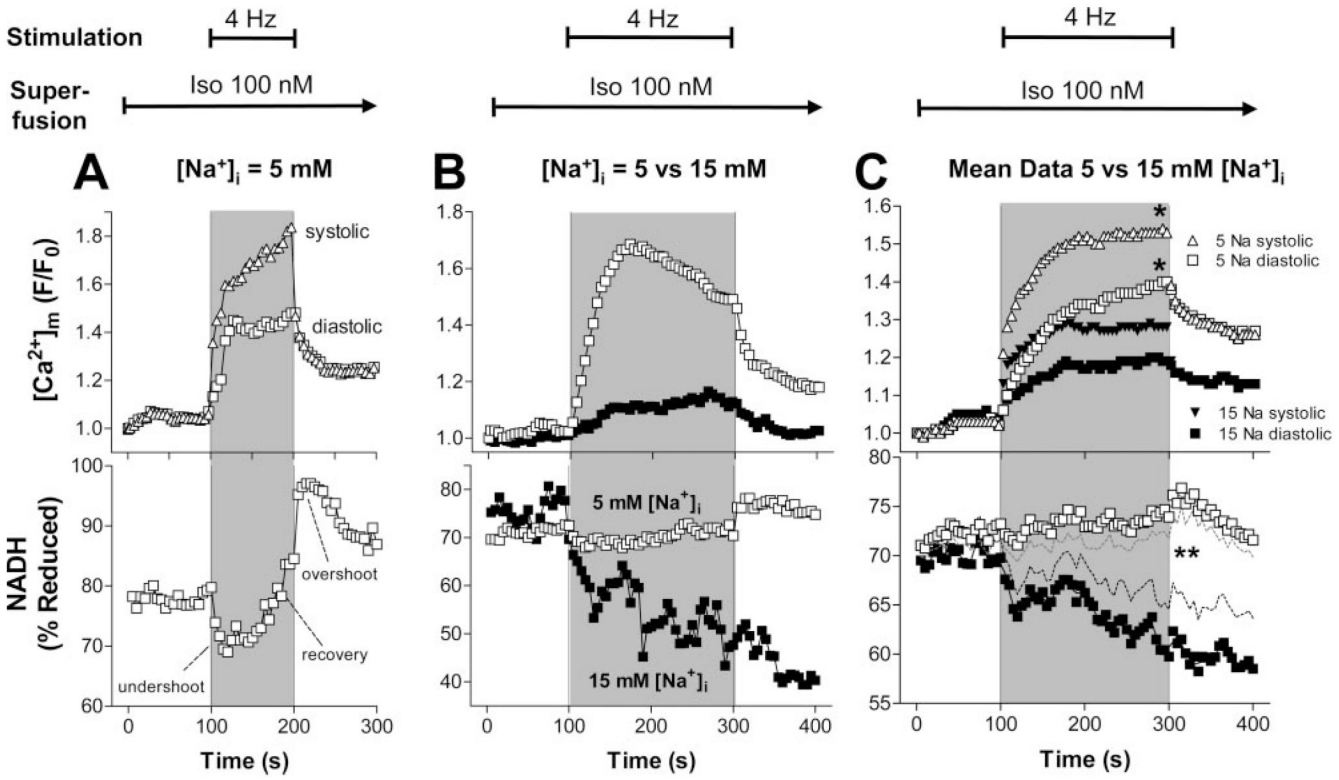

Figure 7.

$[Ca^{2+}]_m$ (upper panels) and NADH (lower panels) in representative cells (A and B) or as aggregate data (C) at 5 or 15 mmol/L $[Na^+]_i$, respectively (C: 5 mmol/L $[Na^+]_i$, n = 16; 15 mmol/L $[Na^+]_i$, n=13). Resting myocytes were held at E_H=−80 mV, and after recording the first data point, were superfused with 100 nmol/L isoproterenol. After 100 seconds, myocytes were pulsed at 4 Hz for 100 seconds (A) or 200 seconds (B and C), respectively. After pacing, cells were held at −80 mV for another 100 seconds. In C, SEM are omitted for clarity (top) or indicated by dashed lines (bottom). *P<0.05, 5 vs 15 mmol/L $[Na^+]_i$.

NIH-PA Author Manuscript
NIH-PA Author Manuscript
NIH-PA Author Manuscript

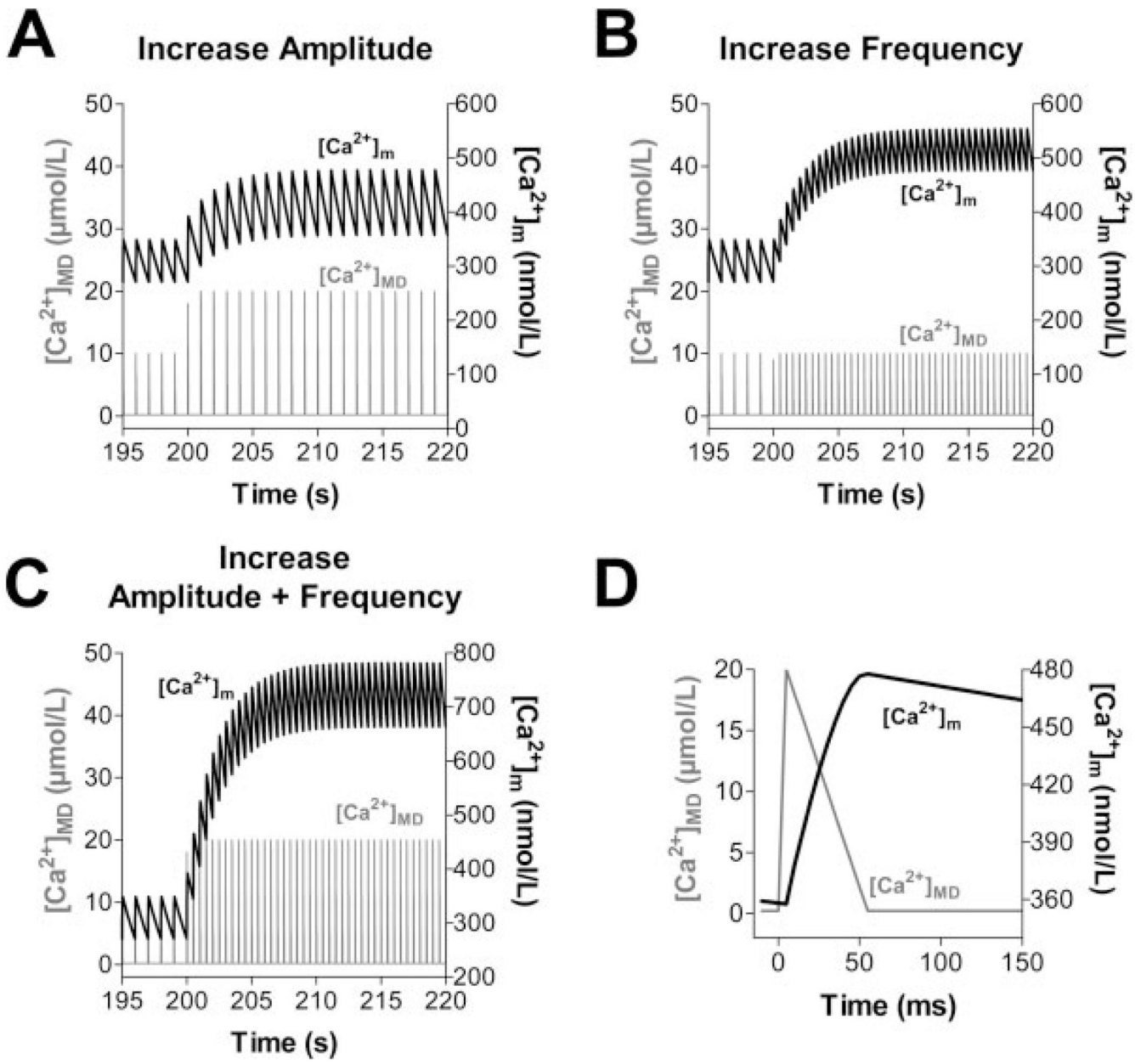

Figure 8.

Computational modeling of $[Ca^{2+}]_m$, assuming a microdomain (MD) in which mitochondria are exposed to $[Ca^{2+}]$ pulses of 10 to 20 µmol/L for 50 ms (D) (representative pulse taken from t=215 s in A). Starting from steady-state conditions with $[Ca^{2+}]_{MD}$ oscillating from 0.1 to 10 µmol/L at 1 Hz, an increase of amplitude (A, from 10 to 20 µmol/L), frequency (B, from 1 to 2 Hz) or both (C) of $[Ca^{2+}]_{MD}$ transients were simulated.